Redox Biology 11 (2017) 30–37

Contents lists available at ScienceDirect

Redox Biology

journal homepage: www.elsevier.com/locate/redox

Research Paper

A new role for oxidative stress in aging: The accelerated aging phenotype in *Sod1*$^{-/-}$ mice is correlated to increased cellular senescence

Yiqiang Zhang[a], Archana Unnikrishnan[e], Sathyaseelan S. Deepa[e], Yuhong Liu[b], Yan Li[b], Yuji Ikeno[c,d], Danuta Sosnowska[e], Holly Van Remmen[f,g], Arlan Richardson[e,g,*]

[a] *Greehy Children's Cancer Institute, The University of Texas Health Science Center at San Antonio, San Antonio, TX, USA*
[b] *Departments of Cellular and Structural Biology, The University of Texas Health Science Center at San Antonio, San Antonio, TX, USA*
[c] *Departments of Pathology, The University of Texas Health Science Center at San Antonio, San Antonio, TX, USA*
[d] *Geriatric Research, Education and Clinical Center (GRECC), South Texas Veterans Health Care System, San Antonio, TX, USA*
[e] *Department of Geriatric Medicine and the Reynolds Oklahoma Center on Aging, Oklahoma University Health Science Center, Oklahoma City, OK, USA*
[f] *Oklahoma Medical Research Foundation, Oklahoma City, OK, USA*
[g] *Oklahoma City VA Medical Center, Oklahoma City, OK, USA*

ARTICLE INFO

Keywords:
Cellular senescence
Superoxide dismutase
Aging
Inflammation
DNA damage
Dietary restriction
Oxidative stress

ABSTRACT

In contrast to other mouse models that are deficient in antioxidant enzymes, mice null for Cu/Zn-superoxide dismutase (*Sod1*$^{-/-}$ mice) show a major decrease in lifespan and several accelerated aging phenotypes. The goal of this study was to determine if cell senescence might be a contributing factor in the accelerated aging phenotype observed in the *Sod1*$^{-/-}$ mice. We focused on kidney because it is a tissue that has been shown to a significant increase in senescent cells with age. The *Sod1*$^{-/-}$ mice are characterized by high levels of DNA oxidation in the kidney, which is attenuated by DR. The kidney of the *Sod1*$^{-/-}$ mice also have higher levels of double strand DNA breaks than wild type (WT) mice. Expression (mRNA and protein) of p16 and p21, two of the markers of cellular senescence, which increased with age, are increased significantly in the kidney of *Sod1*$^{-/-}$ mice as is β-gal staining cells. In addition, the senescence associated secretory phenotype was also increased significantly in the kidney of *Sod1*$^{-/-}$ mice compared to WT mice as measured by the expression of transcripts for IL-6 and IL-1β. Dietary restriction of the *Sod1*$^{-/-}$ mice attenuated the increase in DNA damage, cellular senescence, and expression of IL-6 and IL-1β. Interestingly, the *Sod1*$^{-/-}$ mice showed higher levels of circulating cytokines than WT mice, suggesting that the accelerated aging phenotype shown by the *Sod1*$^{-/-}$ mice could result from increased inflammation arising from an accelerated accumulation of senescent cells. Based on our data with *Sod1*$^{-/-}$ mice, we propose that various bouts of increased oxidative stress over the lifespan of an animal leads to the accumulation of senescent cells. The accumulation of senescent cells in turn leads to increased inflammation, which plays a major role in the loss of function and increased pathology that are hallmark features of aging.

1. Introduction

The Free Radical or Oxidative Stress Theory of Aging postulates that reactive oxygen species (ROS) formed exogenously or endogenously from normal metabolic processes play a role in the aging process. The imbalance of pro-oxidants and antioxidants leads to an age-related accumulation of oxidative damage in macromolecules, resulting in a progressive loss in function and aging [1]. Over the past three decades, the Oxidative Stress Theory of Aging has become one of the most popular theories to explain the biological/molecular mechanism underlying aging because several lines of evidence support the theory. First, the levels of oxidative damage to lipid, DNA, and protein have been reported to increase with age in a wide variety of tissues and animal models [2]. Second, studies with animal models showing increased longevity are consistent with the Oxidative Stress Theory of Aging. Longer-lived animals show reduced oxidative damage and/or increased resistance to oxidative stress, e.g., dietary restriction in rodents and genetic manipulations that increase lifespan in invertebrates (*C. elegans* and *Drosophila*) and in mice [3]. Thus, the observations that experimental manipulations that increase lifespan in invertebrates and rodents were correlated to increased resistance to oxidative stress or reduced oxidative damage provided strong support for the Oxidative

* Corresponding author at: Department of Geriatric Medicine and the Reynolds Oklahoma Center on Aging, University of Oklahoma Health Science Center, Oklahoma City, OK, USA.
E-mail address: Arlan-richardson@ouhsc.edu (A. Richardson).

http://dx.doi.org/10.1016/j.redox.2016.10.014
Received 2 September 2016; Received in revised form 19 October 2016; Accepted 22 October 2016
Available online 02 November 2016

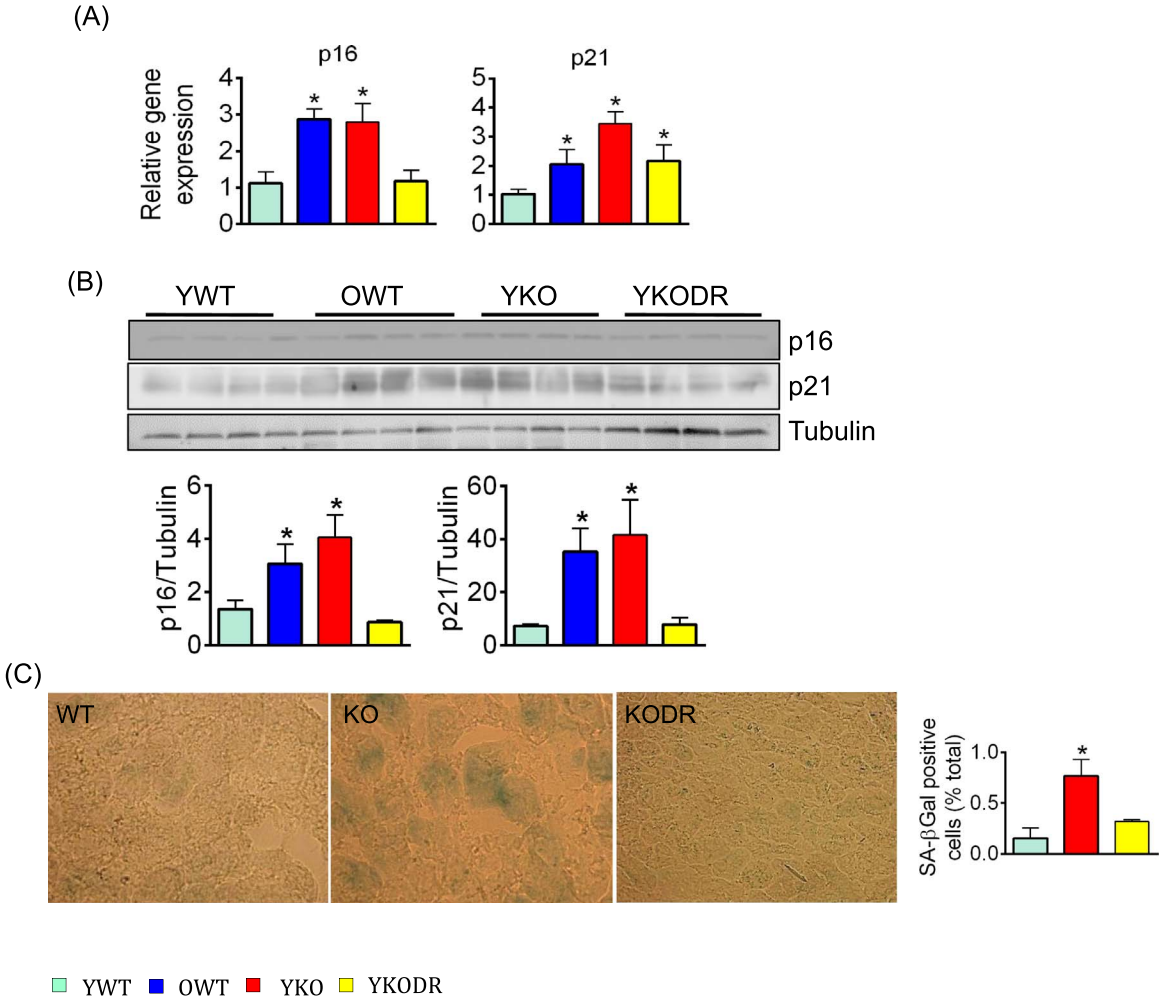

Fig. 1. Cellular senescence is increased in kidney of *Sod1*$^{-/-}$ mice. (A) Transcript levels of p16INK4a and p21 in kidney measured by qRT-PCR and normalized to GAPDH. (B) The level of p16INK4a and p21 protein in kidney as measured by Western blot (top panel). Quantification of p16INK4a and p21 normalized to β-tubulin is shown in the bottom panel. (C) Images of SA β-Gal positive staining cells in kidney is shown in the left panel (arrow points to β-Gal positive cells). Percentage of SA β-Gal positive cells is quantified and graphically represented in the right panel. Four groups of mice were studied: young (4–6 month-old) WT (YWT, turquoise bar); old (24 month-old) mice (OWT, blue bar); young (4–6 month-old) *Sod1*$^{-/-}$ mice (YKO, red bar); young (6-month-old) *Sod1*$^{-/-}$ mice on DR (YKODR, yellow bar). The data are the mean ± SEM of 4 mice per group and were statistically analyzed by one-way ANOVA followed by student T-test. The asterisk (*) indicates a significance ($P < 0.05$) difference between either young WT mice or young *Sod1*$^{-/-}$ mice on DR and old WT mice or young *Sod1*$^{-/-}$ mice on DR. There were no significant differences between the old WT and young *Sod1*$^{-/-}$ mice or the young WT and young DR young *Sod1*$^{-/-}$ mice. (For interpretation of the references to color in this figure legend, the reader is referred to the web version of this article.)

Stress Theory of Aging. However, all of the experimental manipulations that increase lifespan also alter processes other than oxidative stress/damage; therefore, the increase in longevity in these animal models could arise through another mechanism.

Over the past two decades, our group has directly tested the role of oxidative damage/stress in aging by genetically manipulating the antioxidant status of a wide variety of antioxidant genes to increase or reduce the level of oxidative stress/damage and determine what affect these manipulations had on lifespan. Our research with 18 different genetic manipulations in the antioxidant defense system shows that only the mouse model null for Cu/Zn-superoxide dismutase (*Sod1*) had an effect on lifespan (in this case a decrease in lifespan) as predicted by the Oxidative Stress Theory of Aging [4]. Because Elchuri et al. reported that more than 70% of *Sod1*$^{-/-}$ mice developed liver hyperplasia and hepatocellular carcinoma later in life, it was initially believed that the 30% decrease in the lifespan of *Sod1*$^{-/-}$ mice was not due to accelerated aging but was the result of a dramatic increase in hepatocellular carcinoma, which is rare in C57BL/6 mice [5]. In a more recent study, we found a similar 30% decrease in lifespan of the *Sod1*$^{-/-}$ mice; however, in our study, only about 30% of *Sod1*$^{-/-}$ mice developed hepatocellular carcinoma later in life [6]. In addition, we showed that dietary restriction (DR), which is a manipulation that retards aging in rodents, increased the lifespan of the *Sod1*$^{-/-}$ mice to that of normal, wild type (WT) mice. These data combined with studies showing that *Sod1*$^{-/-}$ mice exhibited various accelerated aging phenotypes [e.g., muscle atrophy and loss of fat mass, hearing loss [7], cataracts [8], skin thinning and delayed wound healing [9] lead us to conclude that the *Sod1*$^{-/-}$ mice exhibit accelerated aging. This then raised the question of why we observed a significant decrease in lifespan and accelerated aging in only the *Sod1*$^{-/-}$ mice and not in other mouse models with compromised antioxidant defense systems that showed changes in oxidative stress/damage.

Sod1$^{-/-}$ mice show a much higher level DNA oxidation (i.e., 8-oxo-dG levels) in tissues than any of the mouse models we have studied, which all have deficiencies in one or more of the antioxidant genes [4]. In addition, DNA mutations have been reported to increase significantly in several tissues in *Sod1*$^{-/-}$ mice [10]. Because the DNA damage response has been shown to play a central role in the generation of senescent cells [11] and because Van Deursen's laboratory has shown that clearance of senescent cells delays aging-associated disorders and increases lifespan in a progeroid mouse model [12] as well as normal, WT mice [13], we hypothesized that the increased oxidative damage to DNA in tissues of *Sod1*$^{-/-}$ mice could activate the DNA damage response and drive cells into becoming senescent. To test

our hypothesis, we measured various markers of cellular senescence in kidney tissue, a tissue that shows a significant increase in senescent cells with age [14]. We compared kidney from young-adult and old WT mice and young-adult *Sod1*$^{-/-}$ mice fed *ad libitum* or a DR-diet. Our data clearly demonstrate that the level of senescent cells is dramatically increased in the kidney of young-adult *Sod1*$^{-/-}$ mice compared to young-adult WT mice and are at a level comparable to old WT mice. In addition, we observed that the increase in cellular senescence observed in the *Sod1*$^{-/-}$ mice was attenuated by DR. Interestingly, the increase in cellular senescence in the *Sod1*$^{-/-}$ mice was correlated to increased circulating cytokines. Thus, our data suggest that increased cellular senescence could play a role in the accelerated aging phenotype we have observed in the *Sod1*$^{-/-}$ mice.

2. Results

2.1. Cellular senescence is induced in the kidney of Sod1$^{-/-}$ mice

Using several assays, we measured the level of cell senescence in the kidneys from four groups of mice: 4- to 6- and 24-month-old wild type (WT) mice and 6-month-old *Sod1*$^{-/-}$ mice fed ad libitum or a DR diet. We first measured the expression of two of the well-accepted markers of cellular senescence, p16INK4a and p21 [11]. As shown in Fig. 1A, the transcripts for both p16INK4a and p21 protein increased significantly with age in the WT mice. Berkenkamp et al. had previously reported a 3-fold increase in p16INK4a mRNA levels in the kidney of mice between 3–5 and 18 months of age [14]. More importantly, we observed a 2.5-fold increase in p16INK4a transcript levels in the *Sod1*$^{-/-}$ mice compared to age-matched WT mice, which is similar to the level of p16INK4a in the old WT mice. DR attenuated the increase in cell senescence in the *Sod1*$^{-/-}$ mice. The level of p16INK4a transcripts was significantly reduced in the *Sod1*$^{-/-}$ mice fed a DR diet for 4 months to a level similar to that observed in the young WT mice. As can be seen in Fig. 1A, similar changes were observed in the levels of p21, e.g., the *Sod1*$^{-/-}$ mice showed a 3-fold increase in p21 transcript levels, and DR reduced the expression of p21. We further determined if the changes in p16INK4a and p21 transcript levels were observed at the protein level. Fig. 1B shows the protein levels of p16INK4a and p21 in the kidneys from the four groups of mice. These data show similar changes in the expression of p16INK4a and p21 proteins, i.e., a dramatic increase in these two proteins in the kidneys from old mice and 6-month-old *Sod1*$^{-/-}$ mice, which is reduced by DR. Interestingly in our previous study, we observed no significant difference in p21 levels in liver from 6-month-old WT and *Sod1*$^{-/-}$ mice [6]. We believe that the most likely explanation for these differences in p21 expression in kidney and liver of the *Sod1*$^{-/-}$ mice is due to the physiological differences in how these tissues respond to increased oxidative damage/stress. In liver, increased oxidative stress has been shown to lead to activation of regeneration [15] and increased regenerative proliferation, which is linked to hepatocellular carcinoma [16]. Therefore, Elchuri et al. [5] proposed that oxidative damage/stress in liver results in cell injury/death leading to regeneration, chromosome instability, and eventually hepatocellular carcinoma. Based on our limited data, it would appear that oxidative stress/damage in kidney leads to cell senescence rather than regeneration and proliferation.

We next measured the senescence associated β-galactosidase (SA-β-gal) activity in kidney of *Sod1*$^{-/-}$ mice, which is the hallmark of cellular senescence [17]. As shown in Fig. 2C, very few cells positive for SA-β-gal were observed in the 6-month-old WT mice; however, the number of SA-β-gal positive cells was increased 3.5-fold in the kidney of *Sod1*$^{-/-}$ mice (0.7% vs. 0.2% of the cells were SA-β-gal positive for *Sod1*$^{-/-}$ and wild type mice respectively). Again, DR attenuated the increase of SA-β-gal positive cells in the *Sod1*$^{-/-}$ mice (0.35% of cells were SA-β-gal positive).

We previously reported a significant increase in DNA oxidation (measured as the level of 8-oxo-dG) in several tissues from *Sod1*$^{-/-}$ mice, e.g., skeletal muscle, liver, kidney and brain [7]. To determine if the changes in cell senescence in kidney correlated with changes in DNA damage, we measured the level of 8-oxo-dG in kidney of WT and *Sod1*$^{-/-}$ mice. As shown in Fig. 2A, we observed a significant increase (40%) in DNA oxidative damage in the *Sod1*$^{-/-}$ mice compared to the WT mice, and DR suppressed the increase of DNA oxidation in kidney of the *Sod1*$^{-/-}$ mice to the level observed in the WT mice. In a second cohort of mice, we measured the level of double strand DNA breaks (DSBs) in kidney tissue from 4- month-old WT and *Sod1*$^{-/-}$ mice as percentage of γ-H2AX nuclei, a widely used marker for DSBs [18]. As can be seen in Fig. 2B, kidney from the *Sod1*$^{-/-}$ mice showed a dramatic increase (52%) in DSBs compared to the WT mice. Thus, the increased damage to DNA in the *Sod1*$^{-/-}$ mice is correlated to an accumulation of DSBs in kidney.

2.2. Expression of inflammatory cytokines are induced in the kidney of Sod1$^{-/-}$ mice

Campisi's laboratory made the important discovery that senescent cells secret biologically active proteins (e.g., growth factors, proteases, cytokines, and other factors) that have potent autocrine and paracrine activities [19,20]. Therefore, we measured the expression of several inflammatory cytokines in kidney that have been shown to be induced in senescent cells: IL-6, IL-1β and IL-8. As shown in Fig. 3A, IL-6 and IL-1β transcript levels increased significantly (40-fold and 3-fold respectively) in kidney of old WT mice. Compared to age-matched WT mice, the *Sod1*$^{-/-}$ mice have significantly higher levels of IL-6 and IL-1β mRNA transcripts (20-fold and 2-fold respectively), which are comparable to the transcript levels observed in old WT mice. DR attenuated the increased expression of the transcripts for IL-6 and IL-1β mRNA in the *Sod1*$^{-/-}$ mice. Although we did not observe significant changes in the transcript levels of IL-8 mRNA because of the large animal to animal variation, a trend similar to IL-6 and IL-1β was observed in the old WT and *Sod1*$^{-/-}$ mice for IL-8. In a second group of mice, we also measured the activation of nuclear factor kappa-light-chain-enhancer of activated B cells (NFκB) p65 because cytokines secreted by senescent cells can activate NFκB in surrounding cells, leading to a wave of increased production of pro-inflammatory cytokines in a tissue [21]. The activation of NFκB p65 was measured by the phosphorylated levels of NFκB p65 (pS536) because phosphorylation of this serine residue in the C-terminal transactivation domain has been shown to be involved in nuclear import of p65 to stimulate the expression of specific target genes involved in inflammation. As shown in Fig. 3B, the ratio of NFkB p65 (pS536) to the total NFkB p65 is significantly increased in the *Sod1*$^{-/-}$ mice at both 4 and 9 months of age.

Because we observed changes in the expression of IL-6 in the kidney of the *Sod1*$^{-/-}$ mice, we were interested in determining if circulating levels of IL-6 were increased in the *Sod1*$^{-/-}$ mice. As shown in Fig. 3C, plasma levels of IL-6 increased 4-fold in the old WT mice compared to the young WT. A similar age-related increase in circulating levels of IL-6 has been reported in mice [22]. More importantly, the circulating levels of IL-6 were dramatically increased (over 6-fold) in the *Sod1*$^{-/-}$ mice, and this increase was completely attenuated by DR. Because of the dramatic changes in circulating levels of IL-6 in the *Sod1*$^{-/-}$ mice, we measured the levels of a panel of cytokines in the serum of a second group of 9-month-old WT and *Sod1*$^{-/-}$ mice and 25–29-month-old WT mice. In addition to IL-6, three of the ten cytokines we measured increased significantly in the *Sod1*$^{-/-}$ mice (Table 1). Although we observe a great deal of animal to animal variation in cytokine levels, it is striking that each of the *Sod1*$^{-/-}$ mice showed a global increase in circulating cytokine levels, similar to old WT mice. For example, the sum of the ten cytokine levels was 1.8-fold higher for the *Sod1*$^{-/-}$ mice compared to the WT mice.

2.3. Sod1$^{-/-}$ mice have increased renal pathology

To determine if the changes in cell senescence in the *Sod1*$^{-/-}$ mice had functional consequences, we measured the renal pathology in WT and *Sod1*$^{-/-}$ mice when they died. As shown in Table 2, the overall

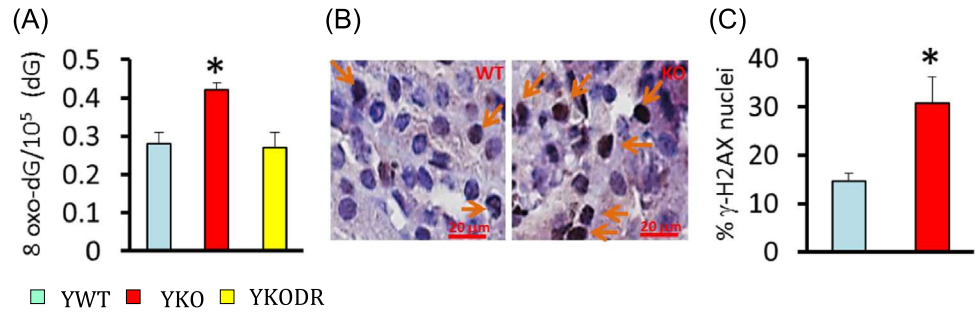

Fig. 2. DNA damage is increased in the kidney of *Sod1*$^{-/-}$ mice. (A) DNA oxidative damage (ratio of 8-oxo-dG to dG). (B) Kidney sections immunostained for γH2AX, a marker for DNA double strand breaks. The arrows point to γH2AX positive nuclei. (C) γH2AX nuclei were quantified, and data shown as mean percentage of nuclei positively stained for γH2AX. The following mice were studied: young (4–6 month-old) WT (turquoise bar); young (4–6 month-old) *Sod1*$^{-/-}$ mice (red bar); young (6-month-old) *Sod1*$^{-/-}$ mice on DR (yellow bar). The DNA oxidative damage data are the mean ± SEM of 4 mice per group and were statistically analyzed by one-way ANOVA followed by student T-test. The asterisk (*) indicates that the values for the *Sod1*$^{-/-}$ mice are significantly different ($P < 0.05$) from the WT mice and DR *Sod1*$^{-/-}$ mice. The DSB data are the mean ± SEM of 4 mice per group and were statistically analyzed by unpaired two-tailed T-test. The asterisk (*) indicates that the values for the *Sod1*$^{-/-}$ mice are significantly different ($P < 0.05$) from the WT mice. (For interpretation of the references to color in this figure legend, the reader is referred to the web version of this article.)

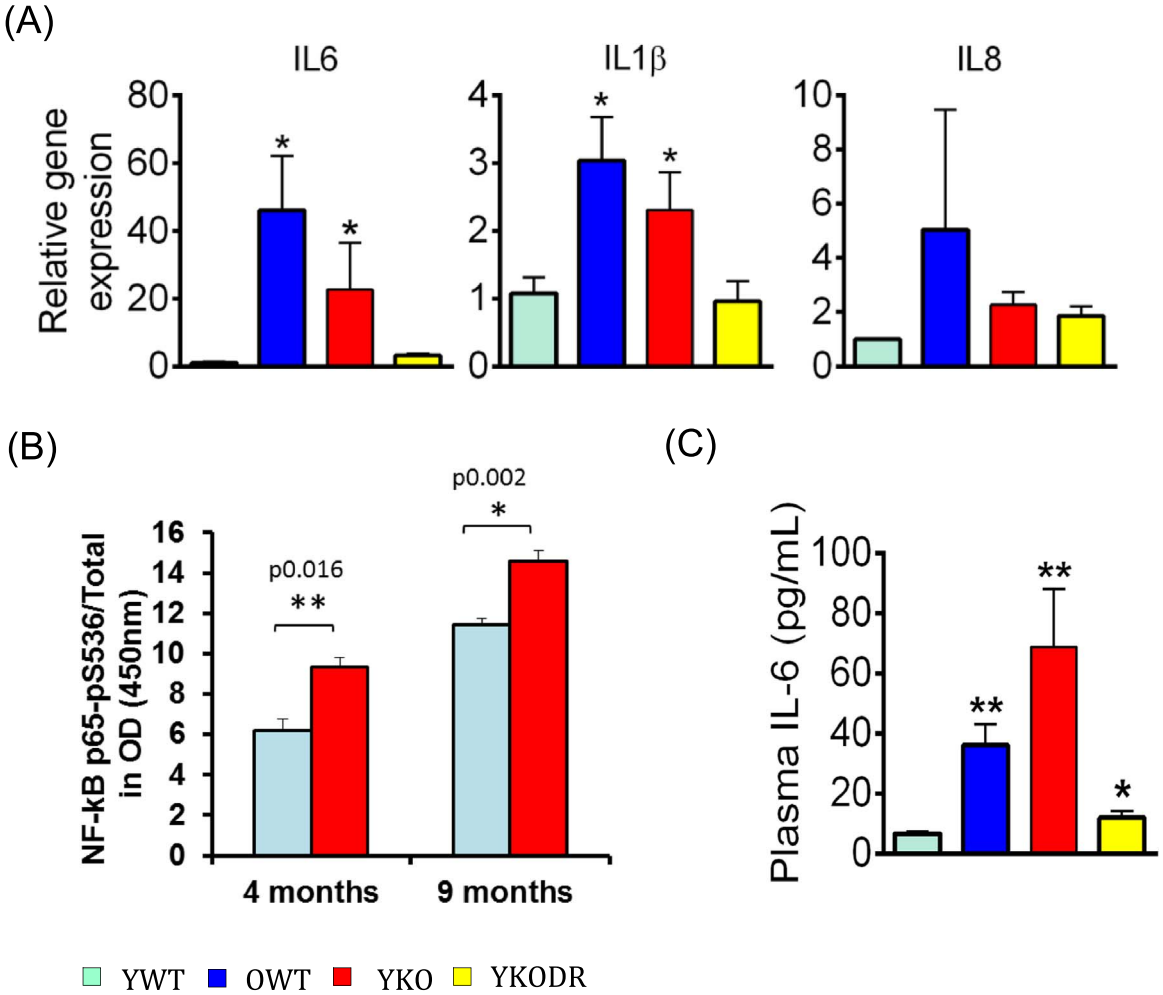

Fig. 3. Expression of inflammatory cytokines are elevated in *Sod1*$^{-/-}$ mice. (A) The levels IL6, IL-1β, and IL-8 mRNA in kidney was measured by qRT-PCR and normalized to GAPDH. (B) NFkB p65 (pS536) levels in kidney were measured using a Simple Step ELISA kit from Abcam [48] and expressed as the ratio of NF-κB p65 pS536/Total NF-κB p65. (C) Quantification of IL-6 in plasma by ELISA. Four groups of mice were studied: young (4–6 month-old) (turquoise bar) and old (24 month-old) mice (blue bar) WT mice and young (4–6 month-old) *Sod1*$^{-/-}$ mice fed ad libitum (red bar) or young (6-month-old) *Sod1*$^{-/-}$ mice on DR (yellow bar). The cytokines data are the mean ± SEM of 4 mice per group and were statistically analyzed by one-way ANOVA followed by student T-test. The asterisks indicate statistical significance (*$P < 0.05$ and **$P < 0.01$) between either young WT mice or young DR *Sod1*$^{-/-}$ mice and old wild type mice or young *Sod1*$^{-/-}$ mice. There were no significant differences between the old WT and young *Sod1*$^{-/-}$ mice or the young WT and young DR *Sod1*$^{-/-}$ mice. The NF-κB p65 (pS536) data are the mean ± SEM of 4 mice per group and were statistically analyzed by unpaired two-tailed T-test. The asterisk (*) indicates that the values for the *Sod1*$^{-/-}$ mice are significantly different ($P < 0.01$) from the WT mice. (For interpretation of the references to color in this figure legend, the reader is referred to the web version of this article.)

Table 1
Cytokine levels in the blood of WT Young, WT Old and *Sod1*$^{-/-}$ mice.

	G-CSF	Eotaxin	GM-CSF	IL-1α	IL-1β	IL-6	KC (IL-8)	MCP-1	MIP-1	TNFα	TOTAL
KO-1	2008	12071	60	227	0	70	752	450	98	27	15763
KO-2	2938	14029	0	959	0	66	689	220	678	0	19579
KO-3	3634	8168	0	1004	100	36	890	828	594	29	15283
KO-4	1686	10007	90	1733	238	0	774	572	594	67	15761
KO-5	4009	7595	109	469	259	45	337	503	0	38	13364
KO-6	2968	11733	0	1766	0	0	794	0	0	33	17294
AVG	**2874***	**10601***	**43**	**1026**	**100**	**36***	**706***	**429**	**327**	**32**	**16174***
SEM	367	1008	20	258	50	13	78	117	133	9	854
P-value	0.003	0.0008	0.08	0.21	0.1	0.05	0.03	0.14	0.47	0.06	0.0009
WT-Old-1	1977	5369	192	538	89	51	621	757	470	34	10098
WT-Old-2	2295	5267	147	758	155	28	543	468	0	24	9685
WT-Old-3	2134	7286	373	1421	0	0	3742	814	1669	75	17514
WT-Old-4	1313	9313	579	3422	0	262	2275	334	2292	0	19790
WT-Old-6	3063	6048	230	1328	156	358	896	612	1160	32	13883
WT-Old-7	0	8852	0	735	0	0	2566	572	98	0	12823
WT-Old-8	1545	5162	0	1065	0	152	3543	0	1578	0	13045
WT-Old-9	2583	6651	0	2067	0	112	1266	0	0	0	12679
AVG	**1864**	**6744***	**190***	**1417**	**50**	**120***	**1932***	**445**	**908***	**21**	**13689***
SEM	311	541	69	315	24	44	428	104	296	9	1148
P-value	0.09	0.04	0.02	0.4	0.2	0.02	0.006	0.1	0.05	0.2	0.002
WT-Young-1	1178	6548	38	661	0	9	260	0	312	0	9006
WT-Young-2	2057	4259	0	1487	0	27	696	302	382	6	9216
WT-Young-3	252	6677	0	1016	0	0	169	438	616	39	9207
WT-Young-4	1433	4465	0	919	87	12	581	394	0	19	7940
WT-Young-5	1273	3628	12	3398	34	11	483	220	382	0	9441
AVG	**1239**	**5115**	**10**	**1496**	**24**	**12**	**438**	**271**	**338**	**13**	**8962**
SEM	290	627	7	493	17	4	98	77	99	7	265

The levels of ten cytokines were measured in the serum collected from five 9-month-old WT (WT-Young), nine 26–29-month-old WT (WT-old) and six 9-month-old *Sod1*$^{-/-}$ (KO) mice. The level of each cytokine is shown for each of the mice studied and is expressed as pg/ml (0 indicates that the level of the cytokine in the serum of that animal was undetectable). The total represents the sum of the levels of all ten cytokines in the serum of each mouse. The data were analyzed using one-tailed student's T-test, and the p-values are given. Cytokines showing a significant increase in the *Sod1*$^{-/-}$ mice and old mice, compared to young-WT, are identified with an asterisk.

Table 2
Renal pathology in WT and *Sod1*$^{-/-}$ mice.

	WT (n=36)	KO (n=50)	KODR (n=47)
Incidence of mice with renal pathology (percent):	25 (69%)	44 (88%)*	33 (70%)
Incidence-free mice (percent):	11 (31%)	6 (12%)*	14 (30%)
Total kidney disease incidence (average score per animal):	24 (0.96)	88 (1.76)*	38 (1.15)
Disease burden expressed as number of lesions per mouse	0.96	1.76*	1.15
Glomerulonephritis			
Total incidence (percent):	20 (56%)	37 (74%)*	26 (55%)
Total severity score (average score per animal?):	27 (1.35)	64 (1.73)**	49 (1.88)

The data presented are end of life pathology that were extrapolated and summarized from previous studies by our group [6,49].

* $p < 0.05$ denotes statistical significance between the KO (*Sod1*$^{-/-}$ mice) and the other two groups, WT (wild type) or KODR (*Sod1*$^{-/-}$ mice on DR).

** $p < 0.05$ denotes significance difference between the KO and WT mice but not the KODR.

renal pathology increased significantly in the kidney of *Sod1*$^{-/-}$ mice, e.g., the incidence of mice with renal pathology is significantly higher in the *Sod1*$^{-/-}$ mice. In addition, the total number of lesions identified in the *Sod1*$^{-/-}$ mice was significantly higher as well as the number of lesions per mouse with renal pathology, which indicates that the severity of renal pathology was significantly greater in *Sod1*$^{-/-}$ mice. The renal pathology lesions that increased most prominently in the *Sod1*$^{-/-}$ mice included glomerulonephritis, nephrocalcinosis, and lymphocyte infiltration. *Sod1*$^{-/-}$ mice maintained on a DR-diet showed a significant reduction in both the incidence and severity of renal pathology.

3. Discussion

The role of oxidative stress in aging has been called into question by experiments from our group showing that in 18 different genetically modified mouse models, in which various components of the antioxidant defense system were altered to increase or decrease the level of oxidative stress/damage in tissues, only *Sod1*$^{-/-}$ mice showed a change in lifespan (a 30% decrease) and accelerated aging phenotypes as predicted by the Oxidative Stress Theory of Aging [23]. The focus of this study was to begin testing various mechanisms that would account for the accelerated aging in the *Sod1*$^{-/-}$ mice. Because DNA oxidation (i.e., 8-oxo-dG levels) is much higher in tissues from the *Sod1*$^{-/-}$ mice than in any of the mouse models we have studied, which all have deficiencies in one or more of the antioxidant genes [4], we hypothesized that the *Sod1*$^{-/-}$ mice might show increased cell senescence. Consistent with this hypothesis, is our observation that DR, which increased the lifespan of *Sod1*$^{-/-}$ mice [6], reduces the level of DNA oxidation in the *Sod1*$^{-/-}$ mice. It is well established that DR dramatically increases the resistance of mice to oxidative stress, leading to reduced oxidative damage to various macromolecules [2], including the level of 8-oxo-dG in DNA of tissues from rats and mice [24]. By itself, 8-oxo-dG is not particularly mutagenic; however, when 8-oxo-dG residues are found in a cluster of lesions along with single strand breaks, double strand DNA breaks (DSBs) are generated when the cell attempts to repair these lesions [25–27]. Our data show that the level of DSBs is significantly increased in the kidney of *Sod1*$^{-/-}$ mice compared to WT mice. Although we did not study the effect of DR on the level of DSBs in Sod1$^{-/-}$ mice, Hallam et al., 2016, showed that the age related increase (~30%) in H2A.X foci in the central cornea of the mice was attenuated by DR [28]. DSBs have been shown to be involved in the generation of senescent cells through the formation of DNA-SCARS (DNA segments with chromatin alterations reinforcing senes-

cence) [29], which are persistent DNA damage foci that induce the DNA damage response signaling including the induction of two tumor suppressor pathways, e.g., p53/p21 and pRB/p16INK4a. Most senescent cells express p16INK4a, which is a cyclin-dependent kinase inhibitor that leads to pRb hypophosphorylation. The expression of p16INK4a has been shown to increase with age in mouse and human [30]. Our data clearly demonstrate that the level of senescent cells is dramatically increased in the kidney of young (6 months) *Sod1*$^{-/-}$ mice compared to young WT mice and is at a level comparable to old (24 months) mice, e.g., an increase in the expression of p16INK4a and p21 and an increase in β-gal positive cells was observed. In addition, the increase in cell senescence observed in the *Sod1*$^{-/-}$ mice was attenuated by DR, which we have shown increases the lifespan of the *Sod1*$^{-/-}$ mice [6]. Thus, we show that the decrease in the lifespan in the *Sod1*$^{-/-}$ mice or the increase in the lifespan of the *Sod1*$^{-/-}$ mice fed a DR diet, correlate to changes in cell senescence. Van Deursen's laboratory has shown that clearance of p16INK4a positive senescent cells delays aging-associated disorders and increases lifespan in a progeroid mouse model as well as normal, WT mice [12,13]. Thus, cell senescence could play a role in the accelerated aging phenotype we have observed in the *Sod1*$^{-/-}$ mice.

Our data also point to a mechanism of how the increase in cell senescence might lead to accelerated aging in the *Sod1*$^{-/-}$ mice. Campisi's laboratory has shown that senescent cells secret biologically active proteins (e.g., growth factors, proteases, cytokines, and other factors) that have potent autocrine and paracrine activities [19]; a process termed the senescence associated secretory phenotype (SASP). The SASP includes several potent inflammatory cytokines including IL-1β, IL-6 and IL-8 which may serve as an important source of low-level chronic inflammation [31]. We showed that the expression of IL-6 and IL-1β are dramatically increased in the kidney of the *Sod1*$^{-/-}$ mice. We also measured the levels of NFκB p65 activation in kidney tissue because cytokines produced by senescent cells have been shown to activate NFκB in surrounding cells. Therefore, only a few senescent cells have the potential to lead to a wave of increased production of pro-inflammatory cytokines in a tissue [21]. The NFkB pathway is a well-established proinflammatory signaling pathway known to increase expression of cytokines and chemokines [32]. We showed that NFκB activation was higher in the kidney of the *Sod1*$^{-/-}$ mice. Because NFkB has been shown to act as a master regulator of the expression of SASP genes [33,34], the increase in NFkB activation in the *Sod1*$^{-/-}$ mice could further increase the production of pro-inflammatory cytokines by senescent cells.

Based on our study with kidney, we propose senescent cells also accumulate in other tissues of the *Sod1*$^{-/-}$ mice, and this accumulation of senescent cells in *Sod1*$^{-/-}$ mice plays a role in the accelerated aging and increased mortality observed in the *Sod1*$^{-/-}$ mice through the production of proinflammatory cytokines by senescent cells. Indeed, we showed that *Sod1*$^{-/-}$ mice had elevated circulating levels of many proinflammatory cytokines, demonstrating for the first time that inflammation is elevated in the *Sod1*$^{-/-}$ mice. Finch and Grimmins argue that senescent cells play an important role in increased inflammation that contributes to aging and age-related disease [35]. Chronic, low grade inflammation with age, often called 'inflammaging' is a prevalent feature of aging as well as many age-related diseases such as cardiovascular disease, type 2 diabetes, and dementia [36]. In addition, inflammaging is a substantial risk factor for both morbidity and mortality in the elderly people, e.g., epidemiological data show that inflammaging is associated with and predictive of aging phenotypes including frailty [36,37].

We recognize that increased oxidative stress in the *Sod1*$^{-/-}$ mice could lead to increased inflammation by mechanisms other than cell senescence. For example, necroptosis is a novel pathway of regulated necrosis that plays an important role in the development of inflammation and inflammatory diseases. Necroptosis can be induced by multiple factors such as death receptors, interferons, toll-like receptors or intracellular RNA, DNA sensors, and recent studies show that oxidative stress is an important initiator of necroptosis [38]. For example, absence of glutathione peroxidase 4 has been shown to induce necroptosis in mouse erythroid precursor cells [39], and knocking out a necrosis mediating protein, RIP3 (receptor-interacting protein 3) reduces inflammation and mortality in a mouse model of atherosclerosis [40,41]. Oxidative stress has also been linked to the development of inflammation through activation of NLRP3 inflammasome. The NLRP3 inflammasome is unique among innate immune sensors because it can be activated in response to a diverse array of endogenous metabolic "danger signals" to induce sterile inflammation in absence of overt infection. The generation of reactive oxygen species is one of the proposed mechanisms that triggers NLPR3 activation [42], and a recent study has shown that reduction of NLRP3 inflammasome activation enhances healthspan and reduces age-related functional decline in mice [43].

In summary, we believe that our data point to a new concept of how oxidative stress might lead to aging. Initially, it was proposed that oxidative damage (e.g., damage to lipid, protein, or DNA) was responsible for a deterioration of cellular function and eventually age-related pathologies and aging. However, cells have numerous pathways to repair damage that occurs to cellular macromolecules, i.e., macromolecular damage represents a steady state between the amount of damage occurring at one time and the ability of cells to repair the damage. Thus, a cell/tissue might experience a high level of oxidative stress resulting in high levels of damage, which could be repaired over time. Based on our data, we propose that in response to high levels of oxidative damage resulting in DSBs, a cell becomes senescent, which is irreversible. Velarde et al. [44] showed increased DSBs and cell senescence in the skin of very young mice null for Mn-superoxide dismutase (Sod2). *Sod2*$^{-/-}$ mice show massive levels of oxidative stress and die within a few days after birth [45]. We propose that a brief high level of oxidative damage could give rise to a senescent cell before it is repaired to steady state levels by the cell. Once generated, the senescent cell would remain in the tissue over the lifespan of the mouse. Thus, various bouts of oxidative stress over the lifespan of an animal has the potential lead to the accumulation of senescent cells even though the steady state levels of damage are increased only transiently. This concept is similar to the role that DNA damage plays in cancer. DNA damage, which can be continuously repaired, becomes important only when it leads to a permanent change in the genome because of a change in the DNA sequence resulting in a mutation. Therefore, we are proposing that oxidative damage plays a role in aging when the damage produced by increased ROS results in the generation of senescent cells, which can accumulate over the lifespan of an animal.

4. Experimental procedures

4.1. Animals

The *Sod1*$^{-/-}$ mice used in this study were generated by Dr. Charles Epstein and Ting-Ting Huang and were genotyped as previously described [5]. *Sod1*$^{-/-}$ mice were fed a standard NIH-31 chow (19.1% protein, 5.8% fat, 62.7% carbohydrate) obtained from Harlan Teklad, Madison, WI (Diet LM485) and were housed 4 mice/cage under barrier conditions in micro-isolator cages on a 12-h dark/light cycle. For tissue collection, animals were sacrificed by CO_2 inhalation followed by cervical dislocation, and the tissues were immediately excised and placed on ice or in liquid nitrogen depending on the procedures performed later. All tissues following collection were stored at −80 °C and analyzed within 30 days. Dietary restriction (DR) was initiated at 2 months of age by feeding the mice 60% of diet (by weight) consumed by the mice fed ad libitum as described previously [6]. All procedures were approved by the Institutional Animal Care and Use Committee at the University of Texas Health Science Center at San

Antonio.

4.2. Western blots

Mouse kidney was homogenized in ice cold RIPA buffer supplemented with a cocktail of inhibitors for proteases and phosphatases (Roche, Indianapolis, IN). Protein concentrations were determined using the BCA reagents from Thermo Scientific (Rockford, IL). Equal amounts of protein were separated by SDS-polyacrylamide gel electrophoresis and transferred to nitrocellulose membrane. Target proteins were detected with the following specific antibodies against: p21 (F-5) and p16INK4a (M-156) from Santa Cruz Biotechnology (Santa Cruz, CA); SOD1 from Assay Designs (Ann Arbor, MI); and β-tubulin from Sigma (St. Louis, MO).

4.3. Quantitative PCR (qPCR)

RNA was extracted from the kidney using the TRI reagent (Invitrogen, Carlsbad, California) following the manufacturer's instructions. Equal amount of RNA was reverse transcribed into cDNA using the iScript kit from Bio-Rad (Hercules, CA). qPCR was performed using the SYBR green reagents in the ABI 7900H system (Life Technologies, Grand Island, NY) using the following primers, and the mRNA transcript levels were normalized to GAPDH.

p16INK4a (forward: 5'- CCCAACGCCCCGAACT-3', reverse: 5'-GCAGAAGAGCTGCTACGTGAA-3')

p21(forward: 5'-GGCAGACCAGCCTGACAGAT-3', reverse: 5'-TTCAGGGTTTTCTCTTGCAGAAG-3')

IL-6 (forward: 5'-TGGTACTCCAGAAGACCAGAGG-3', reverse: 5'-AACGATGATGCACTTGCAGA-3')

IL-8 (forward: 5'-AGAGGCTTTTCATGCTCAACA-3', reverse: 5'-CCATGGGTGAAGGCTACTGT-3')

MCP1 (forward:5'-GGGATCATCTTGCTGGTGAA-3', reverse: 5'-AGGTCCCTGTCATGCTTCTG-3')

IL-1β (forward: 5-AGGTCAAAGGTTTGGAAGCA-3, reverse: 5-TGAAGCAGCTATGGCAACTG-3')

GAPDH (forward: 5'-CCACTTGAAGGGTGGAGCCA-3', reverse: 5'-TCATGGATGACCTTGGCCAG-3').

4.4. SA-β-gal activity

The assay for SA-β-gal activity was performed as described by Debacq-Chainiaux et al. [46]. Freshly harvested kidney was flash-frozen in liquid nitrogen followed by embedding in Tissue-Tek O.C.T. compound (Sakura Finetek USA, Torrance, CA). The tissues were immediately sectioned in a cryostat machine at 10 µm thickness and transferred to glass slides, followed by fixation in 2% formalin at room temperature for 5 min. After washing with PBS 3 times, the slides were incubated with freshly prepared SA-β-Gal activity detection solution (1 mg/ml X-gal, 5 mM Potassium Ferrocyanide, 5 mM Potassium Ferricyanide, 2 mM MgCl2, pH to 6.0) at 37 °C overnight. After the incubation, the tissues were countered stained with 1% eosin for 3 min followed by washing with PBS for 3 times. The SA-β-Gal positive cells were counted under a light microscope. For each mouse, 3 tissue sections with 10 regions (total cell number was more than 1000 for each section) were analyzed for each kidney.

4.5. Quantification of blood cytokines

Blood was collected in heparin coated tubes followed by centrifugation at 1000×g for 10 min at 4 centigrade. Enzyme linked immunosorbent assay (ELISA) was used to determine the level of IL-6 with a 96-well plate precoated with antibodies specific for mouse IL-6 (BioLegend, San Diego, CA). Each sample was assayed in triplicates. A serial dilution of standard mouse IL-6 was included in the assay. The absorbance at 450 nm was measured in a microplate reader within 30 min. In subsequent experiments, the levels of 10 cytokines in serum were determined using the Milliplex Map Kit: Mouse Cytokine/Chemokine Magnetic Bead Panel (EMD Millipore Corporation, Billerica, MA) and a Luminex Bio-Plex 200 system.

4.6. DNA damage

4.6.1. 8-oxo-dG

Oxidative damage to DNA was measured as the level of 8-oxo-deoxyguanosine (8-oxo-dG) using the HPLC approach as described previously [47]. DNA was isolated from tissues by the NaI method using the DNA Extractor WB kit obtained from Wako Chemicals USA, Inc. (Richmond, VA). Results are expressed as the ratio of nanomoles of 8-oxo-dG to 10^5 nmol of 2-deoxyguanosine.

4.6.2. DNA double strand breaks (DSB)

DSBs were measured by immunochemistry as mean percentage of γ-H2AX positively stained nuclei [18]. Briefly, formalin-fixed paraffin embedded Kidney sections were treated according to standard protocols. Anti-histone H2A.XS139pH from Active Motif (Carlsbad, CA) was used as primary antibody at 1:1000 dilution. HRP-conjugated goat anti-rabbit (Santa Cruz Biotechnology, CA) at a dilution of 1:1000 was used as secondary antibody and the HRP activity was detected using a DAB substrate Kit (Invitrogen Thermo fisher scientific).

Acknowledgements

This study was supported by NIH grants to HVR and AR (P01AG020591 and P01AG051442) and an NIH grant to AR and AU (R01 AG045693). AR and HVR are supported by the Senior Research Career Scientist awards from the Department of Veteran Affairs.

References

[1] R.S. Sohal, R. Weindruch, Oxidative stress, caloric restriction, and aging, Science 273 (1996) 59–63.
[2] A. Bokov, A. Chaudhuri, A. Richardson, The role of oxidative damage and stress in aging, Mech. Ageing Dev. 125 (2004) 811–826.
[3] H. Liang, E.J. Masoro, J.F. Nelson, R. Strong, C.A. McMahan, A. Richardson, Genetic mouse models of extended lifespan, Exp. Gerontol. 38 (2003) 1353–1364.
[4] V.I. Perez, A. Bokov, H. Van Remmen, J. Mele, Q. Ran, Y. Ikeno, A. Richardson, Is the oxidative stress theory of aging dead?, Biochim. Biophys. Acta 1790 (2009) 1005–1014.
[5] S. Elchuri, T.D. Oberley, W. Qi, R.S. Eisenstein, L. Jackson Roberts, H. Van Remmen, C.J. Epstein, T.T. Huang, CuZnSOD deficiency leads to persistent and widespread oxidative damage and hepatocarcinogenesis later in life, Oncogene 24 (2005) 367–380.
[6] Y. Zhang, Y. Ikeno, A. Bokov, J. Gelfond, C. Jaramillo, H.M. Zhang, Y. Liu, W. Qi, G. Hubbard, A. Richardson, H.V. Remmen, Dietary restriction attenuates the accelerated aging phenotype of Sod1-/- mice, Free Radic. Biol. Med. (2013).
[7] F.L. Muller, W. Song, Y. Liu, A. Chaudhuri, S. Pieke-Dahl, R. Strong, T.T. Huang, C.J. Epstein, L.J. Roberts 2nd, M. Csete, J.A. Faulkner, H. Van Remmen, Absence of CuZn superoxide dismutase leads to elevated oxidative stress and acceleration of age-dependent skeletal muscle atrophy, Free Radic. Biol. Med. 40 (2006) 1993–2004.
[8] E.M. Olofsson, S.L. Marklund, A. Behndig, Glucose-induced cataract in CuZn-SOD null lenses: an effect of nitric oxide?, Free Radic. Biol. Med. 42 (2007) 1098–1105.
[9] Y. Iuchi, D. Roy, F. Okada, N. Kibe, S. Tsunoda, S. Suzuki, M. Takahashi, H. Yokoyama, J. Yoshitake, S. Kondo, J. Fujii, Spontaneous skin damage and delayed wound healing in SOD1-deficient mice, Mol. Cell Biochem. 341 (2010) 181–194.
[10] R.A. Busuttil, A.M. Garcia, C. Cabrera, A. Rodriguez, Y. Suh, W.H. Kim, T.T. Huang, J. Vijg, Organ-specific increase in mutation accumulation and apoptosis rate in CuZn-superoxide dismutase-deficient mice, Cancer Res. 65 (2005) 11271–11275.
[11] J. Campisi, F. d'Adda di Fagagna, Cellular senescence: when bad things happen to good cells, Nat. Rev. Mol. Cell Biol. 8 (2007) 729–740.
[12] D.J. Baker, T. Wijshake, T. Tchkonia, N.K. LeBrasseur, B.G. Childs, B. van de Sluis, J.L. Kirkland, J.M. van Deursen, Clearance of p16Ink4a-positive senescent cells delays ageing-associated disorders, Nature 479 (2011) 232–236.
[13] D.J. Baker, B.G. Childs, M. Durik, M.E. Wijers, C.J. Sieben, J. Zhong, R.A. Saltness, K.B. Jeganathan, G.C. Verzosa, A. Pezeshki, K. Khazaie, J.D. Miller, J.M. van Deursen, Naturally occurring p16(Ink4a)-positive cells shorten healthy lifespan, Nature 530 (2016) 184–189.
[14] B. Berkenkamp, N. Susnik, A. Baisantry, I. Kuznetsova, C. Jacobi, I. Sorensen-Zender, V. Broecker, H. Haller, A. Melk, R. Schmitt, In vivo and in vitro analysis of age-associated changes and somatic cellular senescence in renal epithelial cells,

PLoS One 9 (2014) e88071.
[15] N. Dragin, M. Smani, S. Arnaud-Dabernat, C. Dubost, I. Moranvillier, P. Costet, J.-Y. Daniel, E. Peuchant, Acute oxidative stress is associated with cell proliferation in the mice liver, FEBS Lett. 580 (2006) 3845–3852.
[16] H. Barash, E.R. Gross, Y. Edrei, E. Ella, A. Israel, I. Cohen, N. Corchia, T. Ben-Moshe, O. Pappo, E. Pikarsky, D. Goldenberg, Y. Shiloh, E. Galun, R. Abramovitch, Accelerated carcinogenesis following liver regeneration is associated with chronic inflammation-induced double-strand breaks, PNAS 107 (2010) 2207–2212.
[17] G.P. Dimri, X. Lee, G. Basile, M. Acosta, G. Scott, C. Roskelley, E.E. Medrano, M. Linskens, I. Rubelj, O. Pereira-Smith, et al., A biomarker that identifies senescent human cells in culture and in aging skin in vivo, Proc. Natl. Acad. Sci. USA 92 (1995) 9363–9367.
[18] R.R. White, B. Milholland, A. Bruin, S. Curran, R.-M. Laberge, H.V. Steeg, J. Campisi, A.Y. Maslov, J. Vijg, Controlled induction of DNA double-strand breaks in the mouse liver induces features of tissue ageing, Nat. Commun. 6 (2014) 6790.
[19] J.P. Coppe, C.K. Patil, F. Rodier, Y. Sun, D.P. Munoz, J. Goldstein, P.S. Nelson, P.Y. Desprez, J. Campisi, Senescence-associated secretory phenotypes reveal cell-nonautonomous functions of oncogenic RAS and the p53 tumor suppressor, PLoS Biol. 6 (2008) 2853–2868.
[20] J.P. Coppe, C.K. Patil, F. Rodier, A. Krtolica, C.M. Beausejour, S. Parrinello, J.G. Hodgson, K. Chin, P.Y. Desprez, J. Campisi, A human-like senescence-associated secretory phenotype is conserved in mouse cells dependent on physiological oxygen, PLoS One 5 (2010) e9188.
[21] S. Parrinello, J.P. Coppe, A. Krtolica, J. Campisi, Stromal-epithelial interactions in aging and cancer: senescent fibroblasts alter epithelial cell differentiation, J. Cell Sci. 118 (2005) 485–496.
[22] R.A. Daynes, B.A. Araneo, W.B. Ershler, C. Maloney, G.Z. Li, S.Y. Ryu, Altered regulation of IL-6 production with normal aging. Possible linkage to the age-associated decline in dehydroepiandrosterone and its sulfated derivative, J. Immunol. 150 (1993) 5219–5230.
[23] D. Harman, Aging: a theory based on free radical and radiation chemistry, J. Gerontol. 11 (1956) 298–300.
[24] M.L. Hamilton, Z. Guo, C.D. Fuller, H. Van Remmen, W. Ward, S.N. Austad, D.A. Troyer, I. Thompson, A. Richardson, A reliable assessment of 8-oxo-2-deoxyguanosine levels in nuclear and mitochondrial DNA using the sodium iodide method to isolate DNA, Nucleic Acids Res. 29 (2001) 2117–2126.
[25] A.G. Georgakilas, Processing of DNA damage clusters in human cells: current status of knowledge, Mol. Biosyst. 4 (2008) 30–35.
[26] M.R. Lieber, The mechanism of double-strand DNA break repair by the non-homologous DNA end-joining pathway, Annu. Rev. Biochem. 79 (2010) 181–211.
[27] T.B. Kryston, A.B. Georgiev, P. Pissis, A.G. Georgakilas, Role of oxidative stress and DNA damage in human carcinogenesis, Mutat. Res. 711 (2011) 193–201.
[28] D. Hallam, T. Wan, G. Saretzki, Dietary restriction mitigates age-related accumulation of DNA damage, but not all changes in mouse corneal epithelium, Exp. Gerontol. 67 (2015) 772–779.
[29] F. Rodier, D.P. Munoz, R. Teachenor, V. Chu, O. Le, D. Bhaumik, J.P. Coppe, E. Campeau, C.M. Beausejour, S.H. Kim, A.R. Davalos, J. Campisi, DNA-SCARS: distinct nuclear structures that sustain damage-induced senescence growth arrest and inflammatory cytokine secretion, J. Cell Sci. 124 (2011) 68–81.
[30] J. Krishnamurthy, C. Torrice, M.R. Ramsey, G.I. Kovalev, K. Al-Regaiey, L. Su, N.E. Sharpless, Ink4a/Arf expression is a biomarker of aging, J. Clin. Invest. 114 (2004) 1299–1307.
[31] H.Y. Chung, M. Cesari, S. Anton, E. Marzetti, S. Giovannini, A.Y. Seo, C. Carter, B.P. Yu, C. Leeuwenburgh, Molecular inflammation: underpinnings of aging and age-related diseases, Ageing Res. Rev. 8 (2009) 18–30.
[32] Toby Lawrence, The Nuclear Factor NF-κB pathway in inflammation, Cold Spring Harb. Perspect. Biol. 1 (2009) a001651.
[33] Y. Chien, C. Scuoppo, X. Wang, X. Fang, B. Balgley, J.E. Bolden, P. Premsrirut, W. Luo, A. Chicas, C.S. Lee, S.C. Kogan, S.W. Lowe, Control of the senescence-associated secretory phenotype by NF-κB promotes senescence and enhances chemosensitivity, Genes Dev. 25 (2011) 2125–2136.
[34] A. Salminen, A. Kauppinen, K. Kaarniranta, Emerging role of NF-κB signaling in the induction of senescence-associated secretory phenotype (SASP), Cell. Signal. 24 (2012) 835–845.
[35] C.E. Finch, E.M. Crimmins, Inflammatory exposure and historical changes in human life-spans, Science 305 (2004) 1736–1739.
[36] C. Franceschi, J. Campisi, Chronic inflammation (inflammaging) and its potential contribution to age-associated diseases, J. Gerontol. Biol. Sci. Med. Sci. 69 (Suppl. 1) (2014) S4–S9.
[37] D. Calcada, D. Vianello, E. Giampieri, C. Sala, G. Castellani, A. de Graaf, B. Kremer, B. van Ommen, E. Feskens, A. Santoro, C. Franceschi, J. Bouwman, The role of low-grade inflammation and metabolic flexibility in aging and nutritional modulation thereof: a systems biology approach, Mech. Ageing Dev. 136–137 (2014) 138–147.
[38] M. Pasparakis, P. Vandenabeele, Necroptosis and its role in inflammation, Nature 517 (2015) 311–320.
[39] O. Canli, Y.B. Alankus, S. Grootjans, N. Vegi, L. Hultner, P.S. Hoppe, T. Schroeder, P. Vandenabeele, G.W. Bornkamm, F.R. Greten, Glutathione peroxidase 4 prevents necroptosis in mouse erythroid precursors, Blood 127 (2016) 139–148.
[40] L. Meng, W. Jin, X. Wang, RIP3-mediated necrotic cell death accelerates systematic inflammation and mortality, Proc. Natl. Acad. Sci. USA 112 (2015) 11007–11012.
[41] T. Zhang, Y. Zhang, M. Cui, L. Jin, Y. Wang, F. Lv, Y. Liu, W. Zheng, H. Shang, J. Zhang, M. Zhang, H. Wu, J. Guo, X. Zhang, X. Hu, C.M. Cao, R.P. Xiao, CaMKII is a RIP3 substrate mediating ischemia- and oxidative stress-induced myocardial necroptosis, Nat. Med. 22 (2016) 175–182.
[42] A. Abderrazak, T. Syrovets, D. Couchie, K. El Hadri, B. Friguet, T. Simmet, M. Rouis, NLRP3 inflammasome: from a danger signal sensor to a regulatory node of oxidative stress and inflammatory diseases, Redox Biol. 4 (2015) 296–307.
[43] Y.H. Youm, R.W. Grant, L.R. McCabe, D.C. Albarado, K.Y. Nguyen, A. Ravussin, P. Pistell, S. Newman, R. Carter, A. Laque, H. Munzberg, C.J. Rosen, D.K. Ingram, J.M. Salbaum, V.D. Dixit, Canonical Nlrp3 inflammasome links systemic low-grade inflammation to functional decline in aging, Cell Metab. 18 (2013) 519–532.
[44] M.C. Velarde, J.M. Flynn, N.U. Day, S. Melov, J. Campisi, Mitochondrial oxidative stress caused by Sod2 deficiency promotes cellular senescence and aging phenotypes in the skin, Aging 4 (2012) 3–12.
[45] S. Melov, P. Coskun, M. Patel, R. Tuinstra, B. Cottrell, A.S. Jun, T.H. Zastawny, M. Dizdaroglu, S.I. Goodman, T.T. Huang, H. Miziorko, C.J. Epstein, D.C. Wallace, Mitochondrial disease in superoxide dismutase 2 mutant mice, Proc. Natl. Acad. Sci. USA 96 (1999) 846–851.
[46] F. Debacq-Chainiaux, J.D. Erusalimsky, J. Campisi, O. Toussaint, Protocols to detect senescence-associated beta-galactosidase (SA-betagal) activity, a biomarker of senescent cells in culture and in vivo, Nat. Protoc. 4 (2009) 1798–1806.
[47] H. Van Remmen, Y. Ikeno, M. Hamilton, M. Pahlavani, N. Wolf, S.R. Thorpe, N.L. Alderson, J.W. Baynes, C.J. Epstein, T.T. Huang, J. Nelson, R. Strong, A. Richardson, Life-long reduction in MnSOD activity results in increased DNA damage and higher incidence of cancer but does not accelerate aging, Physiol. Genom. 16 (2003) 29–37.
[48] D.N. Kroetz, R.M. Allen, M.A. Schaller, C. Cavallaro, T. Ito, S.L. Kunkel, Type I interferon induced epigenetic regulation of macrophages suppresses innate and adaptive immunity in acute respiratory viral infection, PLoS Pathog. 11 (12) (2015) e1005338.
[49] Y. Zhang, Y. Ikeno, Qi Wenbo, A. Chaudhuri, Y. Li, A. Bokov, S.R. Thorpe, J.W. Baynes, C. Epstein, A. Richardson, H. Van Remmen, Mice deficient in both Mn superoxide dismutase and glutathione peroxidase-1 have increased oxidative damage and a greater incidence of pathology but no reduction in longevity, J. Gerontol. Biol. Sci. Med. Sci. 64 (12) (2009) 1212–1220.